Appl. Math. Mech. -Engl. Ed., **40**(12), 1723–1740 (2019)

Applied Mathematics and Mechanics (English Edition)

https://doi.org/10.1007/s10483-019-2545-8

An analytical study of vibration in functionally graded piezoelectric nanoplates: nonlocal strain gradient theory*

Z. SHARIFI[1], R. KHORDAD[2,†], A. GHARAATI[1], G. FOROZANI[1]

1. Department of Physics, Payame Noor University, Tehran 19395-3697, Iran;

2. Department of Physics, College of Science, Yasouj University, Yasouj 75914-353, Iran

(Received Mar. 17, 2019 / Revised Jul. 3, 2019)

Abstract In this paper, we analytically study vibration of functionally graded piezoelectric (FGP) nanoplates based on the nonlocal strain gradient theory. The top and bottom surfaces of the nanoplate are made of PZT-5H and PZT-4, respectively. We employ Hamilton's principle and derive the governing differential equations. Then, we use Navier's solution to obtain the natural frequencies of the FGP nanoplate. In the first step, we compare our results with the obtained results for the piezoelectric nanoplates in the previous studies. In the second step, we neglect the piezoelectric effect and compare our results with those obtained for the functionally graded (FG) nanoplates. Finally, the effects of the FG power index, the nonlocal parameter, the aspect ratio, and the length-to-thickness ratio, and the nanoplate shape on natural frequencies are investigated.

Key words nonlocal strain gradient, nanoplate, functionally graded piezoelectric (FGP)

Chinese Library Classification O343.7
2010 Mathematics Subject Classification 70-08, 74D05

1 Introduction

In the past four decades, microelectromechanical systems have been widely used in engineering. Examples of the systems are beams, plates, shells, and gears. The problem of predicting mechanical properties of nano/micro structures is an important subject in physics and engineering due to their potential applications. With the fast development of technology, the nano/micro structures have received considerable attention of researchers during the last decade[1–5]. The structures have been employed into many areas like actuators, bio-engineering, nanocomposite and nanoelectromechanical devices.

With advances to nanotechnology, nanoelectromechanical systems (NEMSs) have been fabricated and employed in industry due to their superior features. Due to interesting features of NEMSs such as electrical, optical, and other properties, the systems have better applications compared with microelectromechanical systems. In the NEMSs, the size-dependent effect plays an important role[6–8]. The significant size-dependent effect has been authenticated in nanoscale

* Citation: SHARIFI, Z., KHORDAD, R., GHARAATI, A., and FOROZANI, G. An analytical study of vibration in functionally graded piezoelectric nanoplates: nonlocal strain gradient theory. *Applied Mathematics and Mechanics* (*English Edition*), **40**(12), 1723–1740 (2019) https://doi.org/10.1007/s10483-019-2545-8

† Corresponding author, E-mail: rezakh2025@yahoo.com

structures. For example, Li et al.[9] used nonlocal strain gradient models in examining the size-dependent effects on the static and dynamical behaviors of micro/nano structures. Also, Zhu and Li[10] formulated the longitudinal dynamic problem of a size-dependent elasticity rod by utilizing an integral form of the nonlocal strain gradient theory.

There are several methods to study the size-dependent mechanical properties of micro/nano-scale structures. Examples of the methods are continuum mechanical theories, experimental methods, and molecular dynamic (MD) simulations. Hitherto, many authors have used MD simulations, atomistic models, and the classical continuum elasticity theory to determine the mechanical response in the NEMSs. Also, modified continuum models have been extensively used in the studies of nanomechanics[11–12].

The inhomogeneous materials made of at least two constituent phases are called functionally graded materials (FGMs). Both the compositional profile and the material properties of FGMs vary smoothly and continuously[13–15]. FGMs have received tremendous amount of interest in the past few years due to their major potential in applications such as biomedical implants and heat exchanger tubes[14]. Hitherto, many works have been done on FGMs in the last decade. For example, Li et al.[16] studied the bending, buckling, and vibration behaviors of axially functionally graded (FG) nanobeams. The FG nanoplates have been employed in many applications like NEMSs[17–19]. The wave propagation of FG nanoplate under nonlinear thermal loading was studied by Ebrahimi et al.[20]. For more details, the readers can refer to Refs. [21]–[25].

Piezoelectric materials have their excellent properties. The materials can be employed in piezoelectric transducers, ultrasonic, and smart systems and structures[26–29]. The FGM is a kind of piezoelectric materials which is used for removing the stress concentrations and interfacial debonding[30–32].

It is to be noted that the mechanical properties of piezoelectric materials are size dependent. Therefore, we can use various continuum theories to study physical properties of piezoelectric materials. Examples of the theories are the nonlocal strain gradient theory, the surface elasticity, and the couple-stress theory[33–35]. Many works have been performed on the piezoelectric materials using the aforementioned theories[36–47].

Our studies show that, despite some recent investigations on vibration behaviors of functionally graded piezoelectric (FGP) nanoplates, this problem based on the nonlocal strain gradient theory has not been studied so far. Thus, our motivation is to compare this theory with other models and the correctness of this theory.

In this paper, we study the free vibration of an FGP nanoplate based on the nonlocal strain gradient theory. We assume that the electric potential is zero along the edges of the surface electrodes. We use Hamilton's principle and derive the governing equations. Then, we solve analytically the equations and determine the natural frequency of the FGP nanoplate.

2 Theory and model

The nonlocal stress field and strain gradient effects are related by two scale parameters[46]. Thus, the stress field is given by

$$\sigma_{ij} = \sigma_{ij}^{(0)} - \nabla\sigma_{ij}^{(1)}, \tag{1}$$

where $\sigma_{ij}^{(0)}$ and $\sigma_{ij}^{(1)}$ are the zero order (classical stress) and first order stresses, respectively. The stresses correspond to the strain ε_{ij} and the strain gradient $\nabla\varepsilon_{ij}$ as

$$\sigma_{ij}^{(0)} = \int C_{ijkl}\alpha_0(|x-x'|,\zeta_0)\varepsilon'_{kl}(x')\mathrm{d}x', \tag{2}$$

$$\sigma_{ij}^{(1)} = l^2\int C_{ijkl}\alpha_1(|x-x'|,\zeta_1)\nabla\varepsilon'_{kl}(x')\mathrm{d}x'. \tag{3}$$

Here, $\zeta_0 = e_0 a$ and $\zeta_1 = e_1 a$ denote the nonlocal stress effects, C_{ijkl} is the elastic coefficient, and l is the strain gradient parameter.

When the nonlocal functions $\alpha_0(x, x', e_0 a)$ and $\alpha_1(x, x', e_1 a)$ satisfy the developed conditions by Eringen, the constitutive relation of the nonlocal strain gradient theory has the following form:

$$\begin{aligned}&(1-(e_1 a)^2\nabla^2)(1-(e_0 a)^2\nabla^2)\sigma_{ij}\\ =&C_{ijkl}(1-(e_1 a)^2\nabla^2)\varepsilon_{kl} - C_{ijkl}l^2(1-(e_0 a)^2\nabla^2)\nabla^2\varepsilon_{kl}.\end{aligned} \tag{4}$$

Assuming $e_0 = e_1 = e$, we can write the general constitutive relation in Eq. (4) as

$$\left(1-(ea)^2\nabla^2\right)\sigma_{ij} = C_{ijkl}\left(1-l^2\nabla^2\right)\varepsilon_{kl}. \tag{5}$$

In the nonlocal piezoelasticity, the stress tensor and the electric displacement at a point x depend on not only the strain components and electric-field components at the same point but also another point x' of the body. The basic constitutive equations for piezoelectric materials based on the nonlocal strain gradient theory are given by

$$\sigma_{ij} = \int \alpha(|x-x'|,\tau)(C_{ijkl}\varepsilon_{kl}(x') - e_{kij}E_k)\mathrm{d}x', \tag{6}$$

$$D_i = \int \alpha(|x-x'|,\tau)(e_{ikl}\varepsilon_{kl}(x') - \Xi_{ijk}E_k(x'))\mathrm{d}x', \tag{7}$$

where E_i and D_i are the electric field and the electric displacement, respectively. Also, e_{kij} and Ξ_{ijk} are piezoelectric constants and dielectric constants, respectively, $\alpha(|x-x'|,\tau)$ represents the nonlocal modulus, $|x-x'|$ is the distance, and τ is the scale coefficient that includes the small-scale factor. Based on the Eringen model, the constitutive equations (6) and (7) can be simplified to the equivalent differential constitutive equations as follows:

$$\sigma_{ij} - (e_0 a)^2\nabla^2\sigma_{ij} = C_{ijkl}\varepsilon_{kl} - e_{kij}E_k, \tag{8}$$

$$D_i - (e_0 a)^2\nabla^2 D_i = e_{ikl}(1-l^2\nabla^2)\varepsilon_{kl} + \Xi_{ik}E_k. \tag{9}$$

Since we employ the Cartesian coordinates in our calculations, the stress and displacement due to the electric field use the same gradient. It is noted that the integral constitutive equations in this work are simplified as an approximate differential formulation. Recently, Zhu and Li[10] showed that the nonlocal differential and integral elasticity based models may not be equivalent to each other.

2.1 FGMs

Consider a flat FGP nanoscale plate with the length, the width, and the uniform thickness equal to l_a, l_b, and h, respectively (see Fig. 1).

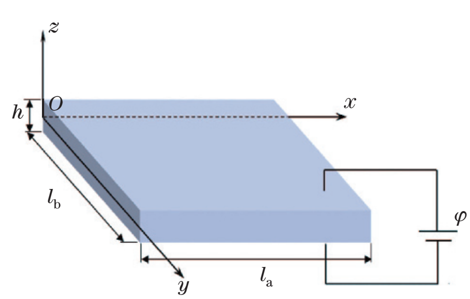

Fig. 1 The geometry of an FGP nanoplate

Consider that the FGP plate is made by the combination of two kinds of piezoelectric materials. Based on the rule of mixture, the effective material property of the FGP plate (P_{eff}) is given by[44]

$$P_{\text{eff}}(z) = P_2 + (P_1 - P_2)\Big(\frac{z}{h} + \frac{1}{2}\Big)^g, \quad 0 \leqslant g \leqslant \infty,$$

where P_1 and P_2 are the bottom and the upper surface properties of the FGP plate, respectively. Also, g is the FG power index.

It should be noted that for $g = 0, P_{\text{eff}} = P_1$, and for $g = \infty, P_{\text{eff}} = P_2$.

3 Governing equations

Based on the Kirchhoff plate theory, one can write the displacement field as

$$u(x, y, z, t) = u_0(x, y, t) - z\frac{\partial w_0(x, y, t)}{\partial x}, \tag{10}$$

$$v(x, y, z, t) = v_0(x, y, t) - z\frac{\partial w_0(x, y, t)}{\partial y}, \tag{11}$$

$$w(x, y, z, t) = w_0(x, y, t), \tag{12}$$

where t is the time, and u_0, v_0, and w_0 are the displacement components in three directions (x, y, and z), respectively. Using the above equations, we can obtain the strains as

$$\varepsilon_{xx} = \frac{\partial u_0}{\partial x} - z\frac{\partial^2 w_0}{\partial x^2}, \tag{13}$$

$$\varepsilon_{yy} = \frac{\partial v_0}{\partial y} - z\frac{\partial^2 w_0}{\partial y^2}, \tag{14}$$

$$\gamma_{xy} = \frac{\partial u_0}{\partial y} + \frac{\partial v_0}{\partial x} - 2z\frac{\partial^2 w_0}{\partial x \partial y}. \tag{15}$$

Moreover, we can obtain[45–47]

$$\phi(x, y, z, t) = -\cos(\beta z)\varphi(x, y, t) + \frac{2V_0}{h} z \mathrm{e}^{\Omega t \mathrm{i}}, \tag{16}$$

where h is the thickness of the piezoelectric plate, $\varphi(x, y, t)$ is the electric potential in the mid-plane, V_0 denotes the amplitude, Ω is the circular excitation frequency, and $\beta = \frac{\pi}{h}$. Applying Eq. (16), one can obtain the electric fields as

$$\begin{cases} E_x = \cos(\beta z)\dfrac{\partial \varphi}{\partial x}, \quad E_y = \cos(\beta z)\dfrac{\partial \varphi}{\partial y}, \\ E_z = -\beta \sin(\beta z)\varphi + \dfrac{2V_0}{h}\mathrm{e}^{\Omega t \mathrm{i}}. \end{cases} \tag{17}$$

Based on the plane-stress assumption, we have $\sigma_{zz}=0$, and our system is a two-dimensional structure. Therefore, the constitutive relations are given by

$$\begin{pmatrix}\sigma_{11}\\ \sigma_{22}\\ \sigma_{33}\\ \sigma_{12}\\ \sigma_{13}\\ \sigma_{23}\end{pmatrix}=\begin{pmatrix}C_{11}&C_{12}&C_{13}&0&0&0\\ C_{12}&C_{11}&C_{13}&0&0&0\\ C_{13}&C_{13}&C_{33}&0&0&0\\ 0&0&0&C_{44}&0&0\\ 0&0&0&0&C_{55}&0\\ 0&0&0&0&0&C_{55}\end{pmatrix}\begin{pmatrix}\varepsilon_{xx}-l^2\nabla^2\varepsilon_{xx}\\ \varepsilon_{yy}-l^2\nabla^2\varepsilon_{yy}\\ \varepsilon_{zz}-l^2\nabla^2\varepsilon_{zz}\\ \gamma_{xy}-l^2\nabla^2\gamma_{xy}\\ \gamma_{xz}-l^2\nabla^2\gamma_{xz}\\ \gamma_{yz}-l^2\nabla^2\gamma_{yz}\end{pmatrix}$$
$$-\begin{pmatrix}0&0&e_{31}\\ 0&0&e_{31}\\ 0&0&e_{33}\\ 0&0&0\\ e_{15}&0&0\\ 0&e_{15}&0\end{pmatrix}\begin{pmatrix}E_1\\ E_2\\ E_3\end{pmatrix}, \tag{18}$$

where $C_{44}=\frac{1}{2}\left(C_{11}-C_{12}\right)$.

Now, using σ_{33} in Eq. (18), we can obtain the following relation:

$$\begin{pmatrix}\sigma_{11}\\ \sigma_{22}\\ \sigma_{12}\\ \sigma_{13}\\ \sigma_{23}\end{pmatrix}=\begin{pmatrix}A&B&0&0&0\\ C&D&0&0&0\\ 0&0&E&0&0\\ 0&0&0&F&0\\ 0&0&0&0&G\end{pmatrix}\begin{pmatrix}\varepsilon_{11}-l^2\nabla^2\varepsilon_{11}\\ \varepsilon_{22}-l^2\nabla^2\varepsilon_{22}\\ \gamma_{12}-l^2\nabla^2\gamma_{12}\\ \gamma_{13}-l^2\nabla^2\gamma_{13}\\ \gamma_{23}-l^2\nabla^2\gamma_{23}\end{pmatrix}-\begin{pmatrix}0&0&e'_{13}\\ 0&0&e'_{23}\\ 0&0&0\\ e_{15}&0&0\\ 0&e_{15}&0\end{pmatrix}\begin{pmatrix}E_1\\ E_2\\ E_3\end{pmatrix}, \tag{19}$$

where

$$e'_{13}=e'_{23}=e_{31}-\frac{C_{13}}{C_{33}}e_{33}, \tag{20}$$

$$A=C_{11}-\frac{C_{13}^2}{C_{33}}=\widetilde{C}_{11},\quad B=C=C_{12}-\frac{C_{13}^2}{C_{33}}=\widetilde{C}_{12},\quad E=F=G=\frac{1}{2}(\widetilde{C}_{11}-\widetilde{C}_{12}). \tag{21}$$

Using the above relations and Eqs. (5) and (6), we can determine the strain constitutive relations for the piezoelectric materials based on the strain gradient theory. The relations are given by

$$\left(1-(e_0a)^2\nabla^2\right)\left(\sigma_{xx}^{(0)}-\nabla\sigma_{xx}^{(1)}\right)=\widetilde{C}_{11}\left(\varepsilon_{xx}-l^2\nabla^2\varepsilon_{xx}\right)+\widetilde{C}_{12}\left(\varepsilon_{yy}-l^2\nabla^2\varepsilon_{yy}\right)-\widetilde{e}_{31}E_z, \tag{22}$$

$$\left(1-(e_0a)^2\nabla^2\right)\left(\sigma_{yy}^{(0)}-\nabla\sigma_{yy}^{(1)}\right)=\widetilde{C}_{12}\left(\varepsilon_{xx}-l^2\nabla^2\varepsilon_{xx}\right)+\widetilde{C}_{11}\left(\varepsilon_{yy}-l^2\nabla^2\varepsilon_{yy}\right)-\widetilde{e}_{31}E_z, \tag{23}$$

$$\left(1-(e_0a)^2\nabla^2\right)\left(\sigma_{xy}^{(0)}-\nabla\sigma_{xy}^{(1)}\right)=\widetilde{C}_{66}\left(\gamma_{xy}-l^2\nabla^2\gamma_{xy}\right), \tag{24}$$

where

$$\widetilde{C}_{66}=\frac{1}{2}\left(\widetilde{C}_{11}-\widetilde{C}_{12}\right),\quad \widetilde{e}_{31}=e_{31}-\frac{C_{13}}{C_{33}}e_{33}. \tag{25}$$

The constitutive relations for electric displacements are given by

$$\begin{pmatrix}D_1\\ D_2\\ D_3\end{pmatrix}=\begin{pmatrix}0&0&0&0&e_{15}&0\\ 0&0&0&0&0&e_{15}\\ e_{31}&e_{31}&e_{33}&0&0&0\end{pmatrix}\begin{pmatrix}\varepsilon_{11}-l^2\nabla^2\varepsilon_{11}\\ \varepsilon_{22}-l^2\nabla^2\varepsilon_{22}\\ \varepsilon_{33}-l^2\nabla^2\varepsilon_{33}\\ \gamma_{12}-l^2\nabla^2\gamma_{12}\\ \gamma_{13}-l^2\nabla^2\gamma_{13}\\ \gamma_{23}-l^2\nabla^2\gamma_{23}\end{pmatrix}+\begin{pmatrix}\Xi_{11}&0&0\\ 0&\Xi_{22}&0\\ 0&0&\Xi_{33}\end{pmatrix}\begin{pmatrix}E_1\\ E_2\\ E_3\end{pmatrix}. \tag{26}$$

Employing previous relations, we now rewrite the following relations:

$$D_x - (e_0 a)^2 \nabla^2 D_x = \Xi_{11} E_x, \tag{27}$$

$$D_y - (e_0 a)^2 \nabla^2 D_y = \Xi_{22} E_y, \tag{28}$$

$$D_z - (e_0 a)^2 \nabla^2 D_z = \widetilde{e}_{31} \left(\varepsilon_{11} - l^2 \nabla^2 \varepsilon_{11}\right) + \widetilde{e}_{31} \left(\varepsilon_{22} - l^2 \nabla^2 \varepsilon_{22}\right) + \widetilde{\widetilde{\Xi}}_{33} E_z, \tag{29}$$

where $\widetilde{\widetilde{\Xi}}_{33} = \Xi_{33} + \frac{e_{33}^2}{C_{33}}$.

The strain energy of the FGP plate using the nonlocal strain gradient theory is given by

$$\begin{aligned} U &= \iiint (\sigma_{ij}\varepsilon_{ij} - D_i E_i)\, \mathrm{d}A\mathrm{d}z \\ &= \iiint (\sigma_{xx}^{(0)} - \nabla\sigma_{xx}^{(1)})\varepsilon_{xx}\mathrm{d}x\mathrm{d}y\mathrm{d}z + \iiint (\sigma_{yy}^{(0)} - \nabla\sigma_{yy}^{(1)})\varepsilon_{yy}\mathrm{d}x\mathrm{d}y\mathrm{d}z \\ &\quad + \iiint (\sigma_{xy}^{(0)} - \nabla\sigma_{xy}^{(1)})\gamma_{xy}\mathrm{d}x\mathrm{d}y\mathrm{d}z - \iiint \big(D_x E_x + D_y E_y + D_z E_z\big)\mathrm{d}x\mathrm{d}y\mathrm{d}z. \end{aligned} \tag{30}$$

Here, it is noted that we have not taken the higher-order stresses $\sigma_{xz}^{(1)}$ and $\sigma_{yz}^{(1)}$ in the strain gradient of the above equations because we have assumed that the size-dependent effects in the thickness direction of the plate are small and thereby we have neglected them. In this regard, recently, Li et al.[9] and Tang et al.[48–49] studied the size-dependent effects in the thickness direction of beams and plates.

Inserting Eqs. (10)–(17) into Eq. (30), we obtain

$$\begin{aligned} U &= \iiint (\sigma_{xx}^{(0)} - \nabla\sigma_{xx}^{(1)})\Big(\frac{\partial u_0}{\partial x} - z\frac{\partial^2 w_0}{\partial x^2}\Big)\mathrm{d}x\mathrm{d}y\mathrm{d}z \\ &\quad + \iiint (\sigma_{yy}^{(0)} - \nabla\sigma_{yy}^{(1)})\Big(\frac{\partial v_0}{\partial y} - z\frac{\partial^2 w_0}{\partial y^2}\Big)\mathrm{d}x\mathrm{d}y\mathrm{d}z \\ &\quad + \iiint (\sigma_{xy}^{(0)} - \nabla\sigma_{xy}^{(1)})\Big(\frac{\partial u_0}{\partial y} + \frac{\partial v_0}{\partial x} - 2z\frac{\partial^2 w_0}{\partial x\partial y}\Big)\mathrm{d}x\mathrm{d}y\mathrm{d}z \\ &\quad - \iiint \Big(D_x\cos(\beta z)\frac{\partial\varphi}{\partial x} + D_y\cos(\beta z)\frac{\partial\varphi}{\partial y} - D_z\beta\sin(\beta z)\varphi - D_z\frac{2V_0}{h}\mathrm{e}^{\Omega t\mathrm{i}}\Big)\mathrm{d}x\mathrm{d}y\mathrm{d}z. \end{aligned} \tag{31}$$

Now, we define the forces and bending moments as

$$(N_x, N_y, N_z) = \int (\sigma_{xx}^{(0)} - \nabla\sigma_{xx}^{(1)}, \sigma_{yy}^{(0)} - \nabla\sigma_{yy}^{(1)}, \sigma_{xy}^{(0)} - \nabla\sigma_{xy}^{(1)})\mathrm{d}z, \tag{32}$$

$$(M_x, M_y, M_z) = \int (\sigma_{xx}^{(0)} - \nabla\sigma_{xx}^{(1)}, \sigma_{yy}^{(0)} - \nabla\sigma_{yy}^{(1)}, \sigma_{xy}^{(0)} - \nabla\sigma_{xy}^{(1)})z\mathrm{d}z. \tag{33}$$

Employing the above equations, the strain energy of the FGP plate can be written as

$$\begin{aligned} U &= \iint \Big(N_x\frac{\partial u_0}{\partial x} + N_y\frac{\partial v_0}{\partial y} + N_{xy}\Big(\frac{\partial u_0}{\partial y} + \frac{\partial v_0}{\partial x}\Big) - M_x\frac{\partial^2 w_0}{\partial x^2} - M_y\frac{\partial^2 w_0}{\partial y^2} - 2M_{xy}\frac{\partial^2 w_0}{\partial x\partial y}\Big)\mathrm{d}x\mathrm{d}y \\ &\quad - \iiint \Big(D_x\cos(\beta z)\frac{\partial\varphi}{\partial x} + D_y\cos(\beta z)\frac{\partial\varphi}{\partial y} - D_z\beta\sin(\beta z)\varphi\Big)\mathrm{d}x\mathrm{d}y\mathrm{d}z. \end{aligned} \tag{34}$$

The kinetic energy of the FGP plate is given by

$$
\begin{aligned}
K &= \iiint \rho(z)\Big(\Big(\frac{\partial u}{\partial t}\Big)^2 + \Big(\frac{\partial v}{\partial t}\Big)^2 + \Big(\frac{\partial w}{\partial t}\Big)^2\Big)\mathrm{d}x\mathrm{d}y\mathrm{d}z \\
&= \iint I_0\Big(\frac{\partial u_0}{\partial t}\frac{\partial u_0}{\partial t} + \frac{\partial v_0}{\partial t}\frac{\partial v_0}{\partial t} + \frac{\partial w_0}{\partial t}\frac{\partial w_0}{\partial t}\Big)\mathrm{d}x\mathrm{d}y \\
&\quad - \iint I_1\Big(\frac{\partial u_0}{\partial t}\frac{\partial^2 w_0}{\partial x\partial t} + \frac{\partial u_0}{\partial t}\frac{\partial^2 w_0}{\partial x\partial t} + \frac{\partial v_0}{\partial t}\frac{\partial^2 w_0}{\partial y\partial t} + \frac{\partial v_0}{\partial t}\frac{\partial^2 w_0}{\partial y\partial t}\Big)\mathrm{d}x\mathrm{d}y \\
&\quad + \iint I_2\Big(\frac{\partial^2 w_0}{\partial x\partial t}\frac{\partial^2 w_0}{\partial x\partial t} + \frac{\partial^2 w_0}{\partial y\partial t}\frac{\partial^2 w_0}{\partial y\partial t}\Big)\mathrm{d}x\mathrm{d}y, \qquad (35)
\end{aligned}
$$

where

$$
(I_0, I_1, I_2) = \int \rho(z)(1, z, z^2)\mathrm{d}z. \qquad (36)
$$

Using Hamilton's principle, i.e., $\int(\delta U - \delta K)\,\mathrm{d}t = 0$, we obtain the following relations:

$$
\frac{\partial N_x}{\partial x} + \frac{\partial N_{xy}}{\partial y} = I_0\ddot{u}_0 - I_1\frac{\partial \ddot{w}_0}{\partial x}, \qquad (37)
$$

$$
\frac{\partial N_y}{\partial y} + \frac{\partial N_{xy}}{\partial x} = I_0\ddot{v}_0 - I_1\frac{\partial \ddot{w}_0}{\partial y}, \qquad (38)
$$

$$
\frac{\partial^2 M_x}{\partial x^2} + \frac{\partial^2 M_y}{\partial y^2} + 2\frac{\partial^2 M_{xy}}{\partial x\partial y} = -I_0\ddot{w}_0 + I_1\Big(\frac{\partial \ddot{u}_0}{\partial x} + \frac{\partial \ddot{v}_0}{\partial y}\Big) - I_2\Big(\frac{\partial^2 \ddot{w}_0}{\partial x^2} + \frac{\partial^2 \ddot{w}_0}{\partial y^2}\Big), \qquad (39)
$$

$$
\int\Big(\frac{\partial D_x}{\partial x}\cos(\beta z) + \frac{\partial D_y}{\partial y}\cos(\beta z) + D_z\beta\sin(\beta z)\Big)\mathrm{d}z = 0. \qquad (40)
$$

Now, we can write the constitutive relations for forces as

$$
N_x - (e_0a)^2\,\nabla^2 N_x = \int \widehat{C}_{11}\left(\varepsilon_{xx} - l^2\nabla^2\varepsilon_{xx}\right)\mathrm{d}z + \int \widehat{C}_{12}\left(\varepsilon_{yy} - l^2\nabla^2\varepsilon_{yy}\right)\mathrm{d}z - \int \widetilde{e}_{31}E_z\mathrm{d}z, \quad (41)
$$

$$
N_y - (e_0a)^2\,\nabla^2 N_y = \int \widehat{C}_{12}\left(\varepsilon_{xx} - l^2\nabla^2\varepsilon_{xx}\right)\mathrm{d}z + \int \widehat{C}_{11}\left(\varepsilon_{yy} - l^2\nabla^2\varepsilon_{yy}\right)\mathrm{d}z - \int \widetilde{e}_{31}E_z\mathrm{d}z, \quad (42)
$$

$$
N_{xy} - (e_0a)^2\,\nabla^2 N_{xy} = \int \frac{1}{2}(\widehat{C}_{11} - \widehat{C}_{12})\left(\gamma_{xy} - l^2\nabla^2\gamma_{xy}\right)\mathrm{d}z. \qquad (43)
$$

Using the following relations:

$$
\nabla^2\varepsilon_{xx} = \frac{\partial^3 u_0}{\partial x^3} - z\frac{\partial^4 w_0}{\partial x^4} + \frac{\partial^3 u_0}{\partial y^2\partial x} - z\frac{\partial^4 w_0}{\partial x^2\partial y^2}, \qquad (44)
$$

$$
\nabla^2\varepsilon_{yy} = \frac{\partial^3 v_0}{\partial y^3} - z\frac{\partial^4 w_0}{\partial y^4} + \frac{\partial^3 v_0}{\partial x^2\partial y} - z\frac{\partial^4 w_0}{\partial x^2\partial y^2}, \qquad (45)
$$

$$
\nabla^2\gamma_{xy} = \frac{\partial^3 v_0}{\partial x^3} + \frac{\partial^3 u_0}{\partial y^3} + \frac{\partial^3 v_0}{\partial y^2\partial x} + \frac{\partial^3 u_0}{\partial x^2\partial y} - 2z\frac{\partial^4 w_0}{\partial x^3\partial y} - 2z\frac{\partial^4 w_0}{\partial y^3\partial x}, \qquad (46)
$$

we have

$$
\begin{aligned}
&N_x-(e_0a)^2\,\nabla^2N_x\\
&=A_{11}\frac{\partial u_0}{\partial x}-B_{11}\frac{\partial^2 w_0}{\partial x^2}-l^2A_{11}\frac{\partial^3 u_0}{\partial x^3}+B_{11}l^2\frac{\partial^4 w_0}{\partial x^4}-l^2A_{11}\frac{\partial^3 u_0}{\partial y^2\partial x}\\
&\quad+l^2B_{11}\frac{\partial^4 w_0}{\partial x^2\partial y^2}+A_{12}\frac{\partial v_0}{\partial y}-B_{12}\frac{\partial^2 w_0}{\partial y^2}-l^2A_{12}\frac{\partial^3 v_0}{\partial x^2\partial y}+l^2B_{12}\frac{\partial^4 w_0}{\partial x^2\partial y^2}\\
&\quad-l^2A_{12}\frac{\partial^3 v_0}{\partial y^3}+l^2B_{12}\frac{\partial^4 w_0}{\partial y^4}+F_{31}\phi, \qquad (47)\\
&N_y-(e_0a)^2\,\nabla^2N_y\\
&=A_{12}\Big(\frac{\partial u_0}{\partial x}-l^2\frac{\partial^3 u_0}{\partial x^3}-l^2\frac{\partial^3 u_0}{\partial y^2\partial x}\Big)-B_{12}\Big(\frac{\partial^2 w_0}{\partial x^2}-l^2\frac{\partial^4 w_0}{\partial x^4}-l^2\frac{\partial^4 w_0}{\partial x^2\partial y^2}\Big)\\
&\quad+A_{11}\Big(\frac{\partial v_0}{\partial y}-l^2\frac{\partial^3 v_0}{\partial y^3}-l^2\frac{\partial^3 v_0}{\partial x^2\partial y}\Big)-B_{11}\Big(\frac{\partial^2 w_0}{\partial y^2}-l^2\frac{\partial^4 w_0}{\partial y^4}-l^2\frac{\partial^4 w_0}{\partial x^2\partial y^2}\Big)+F_{31}\phi, \qquad (48)\\
&N_{xy}-(e_0a)^2\,\nabla^2N_{xy}\\
&=A_{13}\Big(\frac{\partial u_0}{\partial y}+\frac{\partial v_0}{\partial x}-l^2\frac{\partial^3 u_0}{\partial x^2\partial y}-l^2\frac{\partial^3 u_0}{\partial y^3}-l^2\frac{\partial^3 v_0}{\partial x^3}-l^2\frac{\partial^3 v_0}{\partial y^2\partial x}\Big)\\
&\quad-2B_{13}\Big(\frac{\partial^2 w_0}{\partial y\partial x}-l^2\frac{\partial^4 w_0}{\partial x^3\partial y}-l^2\frac{\partial^4 w_0}{\partial x\partial y^3}\Big), \qquad (49)
\end{aligned}
$$

where

$$(A_{11},B_{11},D_{11})=\int\widetilde{C}_{11}(1,z,z^2)\mathrm{d}z, \qquad (50)$$

$$(A_{12},B_{12},D_{12})=\int\widetilde{C}_{12}(1,z,z^2)\mathrm{d}z, \qquad (51)$$

$$(A_{13},B_{13},D_{13})=\int\frac{1}{2}(\widetilde{C}_{11}-\widetilde{C}_{12})(1,z,z^2)\mathrm{d}z, \qquad (52)$$

$$(F_{31},H_{31})=\int\widetilde{e}_{31}(1,z)\beta\sin(\beta z)\mathrm{d}z. \qquad (53)$$

The constitutive relations for moments are given by

$$
\begin{aligned}
&M_x-(e_0a)^2\,\nabla^2M_x\\
&=B_{11}\Big(\frac{\partial u_0}{\partial x}-l^2\frac{\partial^3 u_0}{\partial x^3}-l^2\frac{\partial^3 u_0}{\partial y^2\partial x}\Big)-D_{11}\Big(\frac{\partial^2 w_0}{\partial x^2}-l^2\frac{\partial^4 w_0}{\partial x^4}-l^2\frac{\partial^4 w_0}{\partial x^2\partial y^2}\Big)\\
&\quad+B_{12}\Big(\frac{\partial v_0}{\partial y}-l^2\frac{\partial^3 v_0}{\partial y^3}-l^2\frac{\partial^3 v_0}{\partial x^2\partial y}\Big)-D_{12}\Big(\frac{\partial^2 w_0}{\partial y^2}-l^2\frac{\partial^4 w_0}{\partial y^4}-l^2\frac{\partial^4 w_0}{\partial x^2\partial y^2}\Big)+H_{31}\phi, \qquad (54)\\
&M_y-(e_0a)^2\,\nabla^2M_y\\
&=B_{12}\Big(\frac{\partial u_0}{\partial x}-l^2\frac{\partial^3 v_0}{\partial x^3}-l^2\frac{\partial^3 u_0}{\partial y^2\partial x}\Big)-D_{12}\Big(\frac{\partial^2 w_0}{\partial x^2}-l^2\frac{\partial^4 w_0}{\partial x^4}-l^2\frac{\partial^4 w_0}{\partial x^2\partial y^2}\Big)\\
&\quad+B_{11}\Big(\frac{\partial v_0}{\partial y}-l^2\frac{\partial^3 v_0}{\partial y^3}-l^2\frac{\partial^3 v_0}{\partial x^2\partial y}\Big)-D_{11}\Big(\frac{\partial^2 w_0}{\partial y^2}-l^2\frac{\partial^4 w_0}{\partial y^4}-l^2\frac{\partial^4 w_0}{\partial x^2\partial y^2}\Big)+H_{31}\phi, \qquad (55)
\end{aligned}
$$

$$
\begin{aligned}
&M_{xy}-(e_0a)^2\,\nabla^2 M_{xy}\\
&=B_{13}\Big(\frac{\partial u_0}{\partial y}+\frac{\partial v_0}{\partial x}-l^2\frac{\partial^3 v_0}{\partial x^3}-l^2\frac{\partial^3 u_0}{\partial x^2\partial y}-l^2\frac{\partial^3 u_0}{\partial y^3}-l^2\frac{\partial^3 v_0}{\partial y^2\partial x}\Big)\\
&\quad-2D_{13}\Big(\frac{\partial^2 w_0}{\partial y\partial x}-l^2\frac{\partial^4 w_0}{\partial x^3\partial y}-l^2\frac{\partial^4 w_0}{\partial x\partial y^3}\Big).
\end{aligned}
\tag{56}
$$

The constitutive relations for electric displacements are given by

$$
\int (D_x-(e_0a)^2\nabla^2 D_x)\cos(\beta z)\mathrm{d}z=\int \Xi_{11}\cos^2(\beta z)\frac{\partial\varphi}{\partial z}\mathrm{d}z,
\tag{57}
$$

$$
\int \big(D_y-(e_0a)^2\,\nabla^2 D_y\big)\cos(\beta z)\mathrm{d}z=\int \Xi_{22}\cos^2(\beta z)\frac{\partial\varphi}{\partial z}\mathrm{d}z,
\tag{58}
$$

$$
\begin{aligned}
&\int \big(D_z-(e_0a)^2\,\nabla^2 D_z\big)\beta\sin(\beta z)\mathrm{d}z\\
&=\int \widetilde{e}_{31}\left(\varepsilon_{xx}-l^2\nabla^2\varepsilon_{xx}\right)\beta\sin(\beta z)\mathrm{d}z+\int \widetilde{e}_{31}\left(\varepsilon_{yy}-l^2\nabla^2\varepsilon_{yy}\right)\beta\sin(\beta z)\mathrm{d}z\\
&\quad-\int \widetilde{\Xi}_{33}\beta^2\sin^2(\beta z)\varphi\mathrm{d}z.
\end{aligned}
\tag{59}
$$

Employing the above equations, one can obtain the governing equations of an FGP nanoplate as

$$
\begin{aligned}
&F_{31}\Big(\frac{\partial u_0}{\partial x}+\frac{\partial v_0}{\partial y}-l^2\frac{\partial^3 v_0}{\partial y^3}-l^2\frac{\partial^3 u_0}{\partial y^2\partial x}-l^2\frac{\partial^3 u_0}{\partial x^3}-l^2\frac{\partial^3 v_0}{\partial x^2\partial y}\Big)\\
&-H_{31}\Big(\frac{\partial^2 w_0}{\partial x^2}+\frac{\partial^2 w_0}{\partial y^2}-l^2\frac{\partial^4 w_0}{\partial x^4}-l^2\frac{\partial^4 w_0}{\partial y^4}-2l^2\frac{\partial^4 w_0}{\partial x^2\partial y^2}\Big)-X_{33}\phi+X_{11}\nabla^2\phi=0,
\end{aligned}
\tag{60}
$$

$$
\begin{aligned}
&B_{11}\Big(\frac{\partial^3 u_0}{\partial x^3}-l^2\frac{\partial^5 u_0}{\partial x^5}-2l^2\frac{\partial^5 u_0}{\partial x^3\partial y^2}+\frac{\partial^3 v_0}{\partial y^3}-2l^2\frac{\partial^5 v_0}{\partial x^2\partial y^3}-l^2\frac{\partial^5 v_0}{\partial y^5}+\frac{\partial^3 u_0}{\partial x\partial y^2}+\frac{\partial^3 v_0}{\partial x^2\partial y}\\
&-l^2\frac{\partial^5 v_0}{\partial x^4\partial y}-l^2\frac{\partial^5 u_0}{\partial y^4\partial x}\Big)-D_{11}\Big(\frac{\partial^4 w_0}{\partial x^4}-l^2\frac{\partial^6 w_0}{\partial x^6}-l^2\frac{\partial^6 w_0}{\partial x^4\partial y^2}+\frac{\partial^4 w_0}{\partial y^4}-l^2\frac{\partial^6 w_0}{\partial x^2\partial y^4}-l^2\frac{\partial^6 w_0}{\partial y^6}\\
&+2\frac{\partial^4 w_0}{\partial x^2\partial y^2}-2l^2\frac{\partial^6 w_0}{\partial x^4\partial y^2}-2l^2\frac{\partial^6 w_0}{\partial x^2\partial y^4}\Big)+H_{31}\nabla^2\phi\\
&=\big(1-(e_0a)^2\nabla^2\big)\Big(I_0\ddot{w}_0+I_1\Big(\frac{\partial\ddot{u}_0}{\partial x}+\frac{\partial\ddot{v}_0}{\partial y}\Big)-I_2\Big(\frac{\partial^2\ddot{w}_0}{\partial x^2}+\frac{\partial^2\ddot{w}_0}{\partial y^2}\Big)\Big),
\end{aligned}
\tag{61}
$$

$$
\begin{aligned}
&A_{11}\Big(\frac{\partial^2 u_0}{\partial x\partial y}-l^2\frac{\partial^4 u_0}{\partial x^3\partial y}-l^2\frac{\partial^4 u_0}{\partial y^3\partial x}+\frac{\partial^2 v_0}{\partial y^2}-l^2\frac{\partial^4 v_0}{\partial x^2\partial y^2}-l^2\frac{\partial^4 v_0}{\partial y^4}\Big)\\
&-B_{11}\Big(\frac{\partial^3 w_0}{\partial y^3}-2l^2\frac{\partial^5 w_0}{\partial x^2\partial y^3}-l^2\frac{\partial^5 w_0}{\partial y^5}-l^2\frac{\partial^5 w_0}{\partial x^4\partial y}+\frac{\partial^3 w_0}{\partial x^2\partial y}\Big)+F_{31}\frac{\partial\phi}{\partial y}\\
&+A_{31}\Big(\frac{\partial^2 v_0}{\partial x^2}-\frac{\partial^2 u_0}{\partial x\partial y}+l^2\frac{\partial^4 u_0}{\partial x^3\partial y}+l^2\frac{\partial^4 u_0}{\partial y^3\partial x}-l^2\frac{\partial^4 v_0}{\partial x^4}-l^2\frac{\partial^4 v_0}{\partial x^2\partial y^2}\Big)\\
&=(1-(e_0a)^2\nabla^2)\Big(I_0\ddot{v}_0-I_1\frac{\partial\ddot{w}_0}{\partial y}\Big),
\end{aligned}
\tag{62}
$$

$$
\begin{aligned}
& A_{11}\Big(\frac{\partial^2 u_0}{\partial x^2} - l^2\frac{\partial^4 u_0}{\partial x^2\partial y^2} - l^2\frac{\partial^4 u_0}{\partial x^4} + \frac{\partial^2 v_0}{\partial y\partial x} - l^2\frac{\partial^4 v_0}{\partial x^3\partial y} - l^2\frac{\partial^4 v_0}{\partial x\partial y^3}\Big) \\
& - B_{11}\Big(\frac{\partial^3 w_0}{\partial x^3} - 2l^2\frac{\partial^5 w_0}{\partial x^3\partial y^2} - l^2\frac{\partial^5 w_0}{\partial x^5} - l^2\frac{\partial^5 w_0}{\partial y^4\partial x} + \frac{\partial^3 w_0}{\partial x\partial y^2}\Big) \\
& + A_{13}\Big(\frac{\partial^2 u_0}{\partial y^2} - \frac{\partial^2 v_0}{\partial x\partial y} + l^2\frac{\partial^4 v_0}{\partial x^3\partial y} - l^2\frac{\partial^4 u_0}{\partial y^2\partial x^2} - l^2\frac{\partial^4 u_0}{\partial y^4} + l^2\frac{\partial^4 v_0}{\partial y^3\partial x}\Big) + F_{31}\frac{\partial\phi}{\partial x} \\
= & (1-(e_0a)^2\,\nabla^2)\Big(I_0\ddot{u}_0 - I_1\frac{\partial\ddot{w}_0}{\partial x}\Big). \qquad (63)
\end{aligned}
$$

4 Solution procedures

To solve the above equations, the solutions can be considered as

$$
\begin{pmatrix} u_0 \\ v_0 \\ w_0 \\ \phi \end{pmatrix} = \sum_{m=1}^{\infty}\sum_{n=1}^{\infty}\begin{pmatrix} U_{mn}\cos\Big(\frac{m\pi x}{l_\mathrm{a}}\Big)\sin\Big(\frac{n\pi y}{l_\mathrm{b}}\Big) \\ V_{mn}\cos\Big(\frac{m\pi y}{l_\mathrm{b}}\Big)\sin\Big(\frac{n\pi x}{l_\mathrm{a}}\Big) \\ W_{mn}\sin\Big(\frac{m\pi x}{l_\mathrm{a}}\Big)\sin\Big(\frac{n\pi y}{l_\mathrm{b}}\Big) \\ \phi_{mn}\sin\Big(\frac{m\pi x}{l_\mathrm{a}}\Big)\sin\Big(\frac{n\pi y}{l_\mathrm{b}}\Big) \end{pmatrix}\mathrm{e}^{\omega_{mn}t\mathrm{i}}, \qquad (64)
$$

where ω_{mn} is the circular frequency, and m and n are the half wave numbers. Inserting Eq. (64) into Eqs. (61)–(63), we obtain

$$
\begin{pmatrix} a_{11} & a_{12} & a_{13} & a_{14} \\ a_{21} & a_{22} & a_{23} & a_{24} \\ a_{31} & a_{32} & a_{33} & a_{34} \\ a_{41} & a_{42} & a_{43} & a_{44} \end{pmatrix}\begin{pmatrix} U_{mn} \\ V_{mn} \\ W_{mn} \\ \phi_{mn} \end{pmatrix} = \begin{pmatrix} 0 \\ 0 \\ 0 \\ 0 \end{pmatrix}, \qquad (65)
$$

where

$$
\begin{aligned}
a_{11} = & -A_{11}\Big(\Big(\frac{m\pi}{l_\mathrm{a}}\Big)^2 + l^2\Big(\frac{m\pi}{l_\mathrm{a}}\Big)^4 + l^2\Big(\frac{m\pi}{l_\mathrm{a}}\Big)^4\Big(\frac{n\pi}{l_\mathrm{b}}\Big)^2\Big) - A_{13}\Big(\Big(\frac{n\pi}{l_\mathrm{b}}\Big)^2 + l^2\Big(\frac{n\pi}{l_\mathrm{b}}\Big)^4 \\
& + l^2\Big(\frac{m\pi}{l_\mathrm{a}}\Big)^4\Big(\frac{n\pi}{l_\mathrm{b}}\Big)^2\Big) + I_0\omega_{mn}^2\Big(1+\mu^2\Big(\Big(\frac{m\pi}{l_\mathrm{a}}\Big)^2 + \Big(\frac{n\pi}{l_\mathrm{b}}\Big)^2\Big)\Big), \qquad (66)
\end{aligned}
$$

$$
a_{12} = (A_{13}-A_{11})\Big(\Big(\frac{m\pi}{l_\mathrm{a}}\Big)\Big(\frac{n\pi}{l_\mathrm{b}}\Big) + l^2\Big(\frac{m\pi}{l_\mathrm{a}}\Big)^3\Big(\frac{n\pi}{l_\mathrm{b}}\Big) + l^2\Big(\frac{m\pi}{l_\mathrm{a}}\Big)\Big(\frac{n\pi}{l_\mathrm{b}}\Big)^3\Big), \qquad (67)
$$

$$
a_{13} = F_{31}\Big(\frac{m\pi}{l_\mathrm{a}}\Big), \qquad (68)
$$

$$
\begin{aligned}
a_{14} = & B_{11}\Big(\Big(\frac{m\pi}{l_\mathrm{a}}\Big)^3 + l^2\Big(\frac{m\pi}{l_\mathrm{a}}\Big)^5 + \Big(\frac{m\pi}{l_\mathrm{a}}\Big)\Big(\frac{n\pi}{l_\mathrm{b}}\Big)^2 + 2l^2\Big(\frac{m\pi}{l_\mathrm{a}}\Big)^3\Big(\frac{n\pi}{l_\mathrm{b}}\Big)^2 + l^2\Big(\frac{m\pi}{l_\mathrm{a}}\Big)\Big(\frac{n\pi}{l_\mathrm{b}}\Big)^4\Big) \\
& - I_1\omega_{mn}^2\Big(\frac{m\pi}{l_\mathrm{a}}\Big) - \mu^2 I_1\omega_{mn}^2\Big(\Big(\frac{m\pi}{l_\mathrm{a}}\Big)^3 + \Big(\frac{m\pi}{l_\mathrm{a}}\Big)\Big(\frac{n\pi}{l_\mathrm{b}}\Big)^2\Big), \qquad (69)
\end{aligned}
$$

$$
a_{21} = (A_{13}-A_{11})\Big(\Big(\frac{m\pi}{l_\mathrm{a}}\Big)\Big(\frac{n\pi}{l_\mathrm{b}}\Big) + l^2\Big(\frac{m\pi}{l_\mathrm{a}}\Big)^3\Big(\frac{n\pi}{l_\mathrm{b}}\Big) + l^2\Big(\frac{m\pi}{l_\mathrm{a}}\Big)\Big(\frac{n\pi}{l_\mathrm{b}}\Big)^3\Big), \qquad (70)
$$

$$
\begin{aligned}
a_{22} = & -A_{11}\Big(\Big(\frac{n\pi}{l_\mathrm{b}}\Big)^2 + l^2\Big(\frac{n\pi}{l_\mathrm{b}}\Big)^4 + l^2\Big(\frac{m\pi}{l_\mathrm{a}}\Big)^2\Big(\frac{n\pi}{l_\mathrm{b}}\Big)^2\Big) - A_{13}\Big(\Big(\frac{m\pi}{l_\mathrm{a}}\Big)^2 + l^2\Big(\frac{m\pi}{l_\mathrm{a}}\Big)^4 \\
& + l^2\Big(\frac{m\pi}{l_\mathrm{a}}\Big)^2\Big(\frac{n\pi}{l_\mathrm{b}}\Big)^2\Big) + I_0\omega_{mn}^2\Big(1+\mu^2\Big(\Big(\frac{m\pi}{l_\mathrm{a}}\Big)^2 + \Big(\frac{n\pi}{l_\mathrm{b}}\Big)^2\Big)\Big), \qquad (71)
\end{aligned}
$$

$$a_{23} = F_{31}\Big(\frac{n\pi}{l_{\rm b}}\Big), \tag{72}$$

$$a_{24} = B_{11}\Big(\Big(\frac{n\pi}{l_{\rm b}}\Big)^3 + \Big(\frac{n\pi}{l_{\rm b}}\Big)\Big(\frac{m\pi}{l_{\rm a}}\Big)^2 + l^2\Big(\frac{n\pi}{l_{\rm b}}\Big)^5 + 2l^2\Big(\frac{m\pi}{l_{\rm a}}\Big)^2\Big(\frac{n\pi}{l_{\rm b}}\Big)^3 + l^2\Big(\frac{n\pi}{l_{\rm b}}\Big)\Big(\frac{m\pi}{l_{\rm a}}\Big)^4\Big)$$
$$- I_1\omega_{mn}^2\Big(\frac{n\pi}{l_{\rm b}}\Big) - \mu^2 I_1\omega_{mn}^2\Big(\Big(\frac{n\pi}{l_{\rm b}}\Big)^3 + \Big(\frac{n\pi}{l_{\rm b}}\Big)\Big(\frac{m\pi}{l_{\rm a}}\Big)^2\Big), \tag{73}$$

$$a_{31} = B_{11}\Big(\Big(\frac{m\pi}{l_{\rm a}}\Big)^3 + \Big(\frac{m\pi}{l_{\rm a}}\Big)\Big(\frac{n\pi}{l_{\rm b}}\Big)^2 + l^2\Big(\frac{m\pi}{l_{\rm a}}\Big)^5 + 2l^2\Big(\frac{n\pi}{l_{\rm b}}\Big)^2\Big(\frac{m\pi}{l_{\rm a}}\Big)^3 + l^2\Big(\frac{m\pi}{l_{\rm a}}\Big)\Big(\frac{n\pi}{l_{\rm b}}\Big)^4\Big)$$
$$- I_1\omega_{mn}^2\Big(\frac{m\pi}{l_{\rm a}}\Big) - \mu^2 I_1\omega_{mn}^2\Big(\Big(\frac{m\pi}{l_{\rm a}}\Big)^3 + \Big(\frac{m\pi}{l_{\rm a}}\Big)\Big(\frac{n\pi}{l_{\rm b}}\Big)^2\Big), \tag{74}$$

$$a_{32} = B_{11}\Big(\Big(\frac{n\pi}{l_{\rm b}}\Big)^3 + \Big(\frac{n\pi}{l_{\rm b}}\Big)\Big(\frac{m\pi}{l_{\rm a}}\Big)^2 + l^2\Big(\frac{n\pi}{l_{\rm b}}\Big)^5 + 2l^2\Big(\frac{m\pi}{l_{\rm a}}\Big)^2\Big(\frac{n\pi}{l_{\rm b}}\Big)^3 + l^2\Big(\frac{n\pi}{l_{\rm b}}\Big)\Big(\frac{m\pi}{l_{\rm a}}\Big)^4\Big)$$
$$- I_1\omega_{mn}^2\Big(\frac{n\pi}{l_{\rm b}}\Big) - \mu^2 I_1\omega_{mn}^2\Big(\Big(\frac{n\pi}{l_{\rm b}}\Big)^3 + \Big(\frac{n\pi}{l_{\rm b}}\Big)\Big(\frac{m\pi}{l_{\rm a}}\Big)^2\Big), \tag{75}$$

$$a_{33} = -H_{31}\Big(\Big(\frac{m\pi}{l_{\rm a}}\Big)^2 + \Big(\frac{n\pi}{l_{\rm b}}\Big)^2\Big), \tag{76}$$

$$a_{34} = -D_{11}\Big(\Big(\Big(\frac{m\pi}{l_{\rm a}}\Big)^2 + \Big(\frac{n\pi}{l_{\rm b}}\Big)^2\Big)^2 + l^2\Big(\Big(\frac{m\pi}{l_{\rm a}}\Big)^6 + \Big(\frac{n\pi}{l_{\rm b}}\Big)^6\Big) + 3l^2\Big(\frac{m\pi}{l_{\rm a}}\Big)^4\Big(\frac{n\pi}{l_{\rm b}}\Big)^2$$
$$+ 3l^2\Big(\frac{n\pi}{l_{\rm b}}\Big)^4\Big(\frac{m\pi}{l_{\rm a}}\Big)^2\Big) + I_0\omega_{mn}^2\Big(1 + \mu^2\Big(\Big(\frac{m\pi}{l_{\rm a}}\Big)^2 + \Big(\frac{n\pi}{l_{\rm b}}\Big)^2\Big)\Big)$$
$$+ I_2\omega_{mn}^2\Big(\Big(\frac{m\pi}{l_{\rm a}}\Big)^2 + \Big(\frac{n\pi}{l_{\rm b}}\Big)^2 + \mu^2\Big(\Big(\frac{m\pi}{l_{\rm a}}\Big)^2 + \Big(\frac{n\pi}{l_{\rm b}}\Big)^2\Big)^2\Big), \tag{77}$$

$$a_{41} = -F_{31}\Big(\frac{m\pi}{l_{\rm a}}\Big)\Big(1 + l^2\Big(\Big(\frac{m\pi}{l_{\rm a}}\Big)^2 + \Big(\frac{n\pi}{l_{\rm b}}\Big)^2\Big)\Big), \tag{78}$$

$$a_{42} = -F_{31}\Big(\frac{n\pi}{l_{\rm b}}\Big)\Big(1 + l^2\Big(\Big(\frac{m\pi}{l_{\rm a}}\Big)^2 + \Big(\frac{n\pi}{l_{\rm b}}\Big)^2\Big)\Big), \tag{79}$$

$$a_{43} = -X_{11}\Big(\Big(\frac{m\pi}{l_{\rm a}}\Big)^2 + \Big(\frac{n\pi}{l_{\rm b}}\Big)^2\Big) - X_{33}, \tag{80}$$

$$a_{44} = H_{31}\Big(\Big(\frac{m\pi}{l_{\rm a}}\Big)^2 + \Big(\frac{n\pi}{l_{\rm b}}\Big)^2 + l^2\Big(\Big(\frac{m\pi}{l_{\rm a}}\Big)^2 + \Big(\frac{n\pi}{l_{\rm b}}\Big)^2\Big)^2\Big). \tag{81}$$

5 Results and discussion

Here, we have carried out our analytical calculations for the dimensionless natural frequency $\Omega = \omega l_{\rm a}\sqrt{\big(\frac{I_0}{A_{11}}\big)_{\text{PZT-4}}}$ of an FGP nanoplate by considering various parameters. For this purpose, we have considered an FGP nanoplate consisting of two-phase graded piezoelectric materials such as PZT-4 and PZT-5H. The top and bottom surfaces are PZT-5H and PZT-4, respectively. The material properties are listed in Table 1.

Table 1 Material properties of PZT-4 and PZT-5H

Material	C_{11}/ GPa	C_{12}/ GPa	C_{13}/ GPa	C_{33}/ GPa	e_{31}/ (C·m^{-2})	e_{33}/ (C·m^{-2})	Ξ_{11}/ (C·V^{-1}·m^{-1})	Ξ_{33}/ (C·V^{-1}·m^{-1})	ρ/ (kg·m^{-3})
PZT-4	132	71	73	115	−4.1	14.1	5.841×10^{-9}	7.124×10^{-9}	7 500
PZT-5H	127	80	85	117	−6.62	23.2	15×10^{-9}	13×10^{-9}	7 600

In the first step, to check the present results, we have presented our results for the piezoelectric nanoplate by setting $g = 0$. The first four dimensionless frequencies of the piezoelectric nanoplate for different values of the nonlocal parameter $\mu = e_0a/l_a$ are listed in Table 2. In the table, we can compare our results with those of Refs. [44] and [50]. It is seen from the table that our results are in good agreement with those of Refs. [44] and [50]. It is observed that the natural frequencies are reduced with enhancing the nonlocal parameter for four dimensionless frequencies. The reason for this behavior is the decrease in the stiffness of nanostructures by increasing the nonlocal parameter.

Table 2 Comparisons of the dimensionless natural frequencies of the FGP nanoscale plate for $g = 0$

Frequency	$\mu = 0.0$	$\mu = 0.1$	$\mu = 0.2$	$\mu = 0.3$	$\mu = 0.4$	$\mu = 0.5$
Ω_{11}, present	0.663 2	0.606 0	0.495 6	0.397 9	0.325 3	0.272 3
Ω_{11}, Ref. [50]	0.663 4	0.606 3	0.495 9	0.398 1	0.325 3	0.272 3
Ω_{11}, Ref. [44]	0.662 9	0.605 8	0.495 5	0.397 8	0.325 1	0.272 1
Ω_{12}, present	1.642 0	1.342 7	0.950 6	0.705 3	0.550 5	0.450 8
Ω_{12}, Ref. [50]	1.651 8	1.351 7	0.957 9	0.708 1	0.553 8	0.452 3
Ω_{12}, Ref. [44]	1.631 8	1.335 3	0.946 3	0.699 5	0.547 1	0.446 8
Ω_{22}, present	2.614 9	1.946 1	1.284 9	0.919 8	0.707 0	0.571 2
Ω_{22}, Ref. [50]	2.632 8	1.968 1	1.291 1	0.924 7	0.713 0	0.578 1
Ω_{22}, Ref. [44]	2.571 9	1.922 6	1.261 3	0.903 3	0.696 6	0.564 8
Ω_{13}, present	3.255 3	2.290 8	1.457 2	1.033 6	0.790 2	0.638 4
Ω_{13}, Ref. [50]	3.283 9	2.329 0	1.475 9	1.044 3	0.801 2	0.647 9
Ω_{13}, Ref. [44]	3.183 6	2.258 5	1.431 2	1.012 7	0.776 9	0.628 3

In the second step, we ignore the piezoelectric effect and compare our results with those obtained by Natarajan et al.[50] for the FG nanoplate in Table 3. For this goal, we have considered an FG nanoplate including two-phase graded materials as silicon nitride (Si_3N_4) and stainless steel (SUS304). The used parameters for Si_3N_4 are $\rho_c = 2\ 370$ kg/m^3, $E_c = 348.43 \times 10^9$N/m^2 and for SUS304 are $\rho_m = 8\ 166$ kg/m^3, $E_m = 201.04 \times 10^9$ N/m^2. In Table 3, we have reported the obtained dimensionless fundamental frequency $\Omega = \omega h\sqrt{\frac{\rho_c}{G_c}}$ and compared it with Refs. [44] and [50]. It is clear from Table 3 that our results are in agreement with those of Refs. [44] and [50].

Table 3 Comparisons of the dimensionless natural frequencies of the FG nanoplate for $g = 0$

l_a/l_b	l_a/h	$(e_0a)^2$	Ω_{11}			Ω_{12}			Ω_{22}		
			Present	Ref. [50]	Ref. [44]	Present	Ref. [50]	Ref. [44]	Present	Ref. [50]	Ref. [44]
1	10	0	0.044 6	0.044 1	0.045 8	0.108 9	0.105 1	0.112 7	0.106 2	0.105 1	0.095 5
		1	0.041 0	0.040 3	0.042 0	0.089 5	0.086 0	0.093 4	0.087 1	0.086 0	0.087 5
		2	0.038 2	0.037 4	0.039 0	0.080 2	0.074 5	0.081 4	0.080 2	0.074 6	0.081 3
		4	0.033 4	0.033 0	0.034 5	0.062 5	0.060 9	0.067 0	0.061 5	0.061 0	0.062 4
1	20	0	0.011 4	0.011 3	0.011 5	0.028 1	0.027 8	0.028 6	0.025 6	0.027 9	0.024 0
		1	0.010 2	0.010 3	0.009 8	0.023 3	0.022 8	0.023 5	0.022 2	0.022 8	0.022 0
		2	0.009 6	0.009 6	0.009 8	0.020 2	0.019 7	0.020 4	0.020 1	0.019 8	0.020 4
		4	0.008 4	0.008 5	0.008 6	0.016 5	0.016 1	0.016 7	0.017 2	0.016 2	0.018 0
2	10	0	0.106 9	0.105 5	0.112 7	0.169 1	0.161 5	0.179 5	0.240 5	0.243 0	0.236 0
		1	0.088 3	0.086 3	0.093 4	0.130 2	0.120 8	0.137 6	0.178 9	0.163 7	0.195 7
		2	0.075 1	0.074 8	0.081 4	0.105 9	0.100 6	0.115 8	0.155 1	0.131 0	0.170 8
		4	0.062 4	0.061 2	0.067 0	0.085 5	0.079 3	0.092 0	0.121 2	0.099 9	0.140 6
2	20	0	0.028 2	0.027 9	0.028 6	0.045 3	0.044 0	0.045 8	0.071 1	0.070 1	0.074 4
		1	0.023 3	0.022 9	0.023 5	0.033 6	0.032 9	0.034 5	0.048 9	0.046 4	0.049 9
		2	0.020 1	0.019 8	0.020 4	0.279 0	0.274 0	0.028 8	0.039 8	0.037 1	0.040 1
		4	0.016 3	0.016 2	0.016 7	0.022 0	0.021 6	0.022 7	0.029 7	0.028 3	0.030 6

Figure 2 shows the dimensionless natural frequencies of an FGP nanoplate as a function of the length l_a for three different values of the FG power index with $e_0a = 1$. It is observed from the figure that the natural frequency is reduced by enhancing the length of the nanoplate for all modes. Also, the natural frequency is increased with enhancing the FG power index for a fixed length.

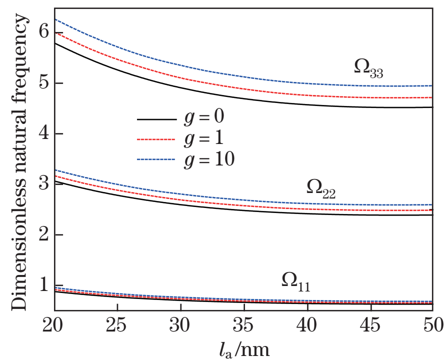

Fig. 2 The dimensionless natural frequency as a function of plate side length for different values of the power index with $e_0a = 1$ (color online)

In Figs. 3(a) and 3(b), we have plotted the dimensionless natural frequency of the FGP nanoplate as a function of the aspect ratio $l_\mathrm{a}/l_\mathrm{b}$ for different values of FG power index with $e_0a = 3$. The natural frequency is increased with the aspect ratio. In addition, the natural frequency is increased with the FG power index for an aspect ratio.

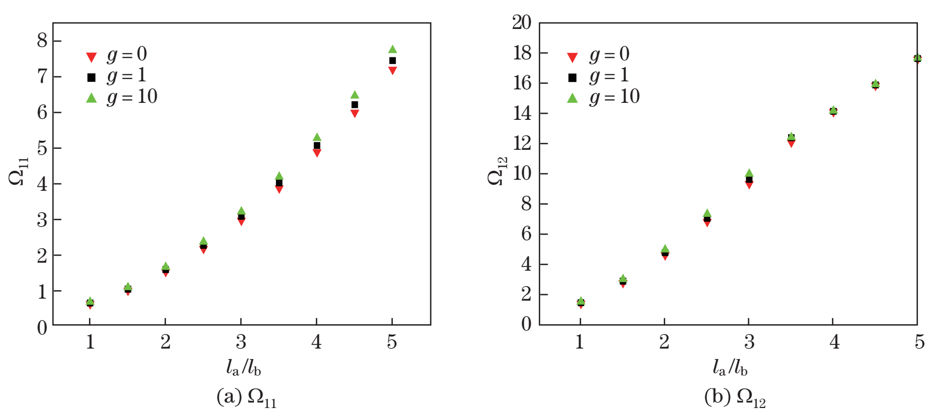

Fig. 3 The dimensionless natural frequency versus the aspect ratio $l_\mathrm{a}/l_\mathrm{b}$ for different values of the power index (color online)

In Figs. 4(a) and 4(b), we have presented the dimensionless natural frequency of the FGP nanoplate versus the length-to-thickness ratio (l_a/h) for three different values of the FG power index and two values of the nonlocal parameters. In the figure, we have selected the length and the width equal to $l_\mathrm{a} = l_\mathrm{b} = 50$ nm while the thickness varies. It is seen from the figures that the dimensionless natural frequency is reduced with l_a/h for two nonlocal parameters. It is noted that, with enhancing l_a/h, the nanoplate becomes thinner and thus it has a lesser stiffness.

In Figs. 5(a) and 5(b), the dimensionless natural frequency ($f_{44} = \Omega_{44}$) is plotted as a function of the FG power index for different values of the strain gradient effect l and the nonlocal parameter μ. It is seen that the dimensionless natural frequency is increased with the strain gradient effect for the fixed nonlocal parameter. Also, by increasing the nonlocal parameter, the values of the dimensionless natural frequency are decreased for the fixed strain gradient effect.

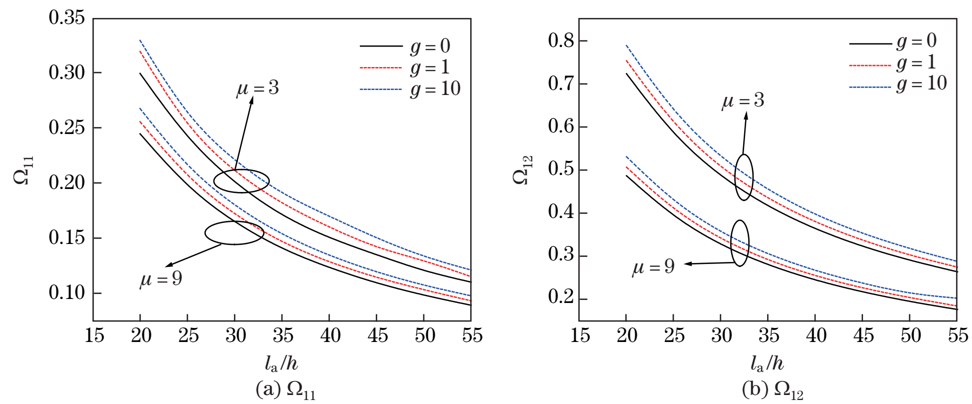

Fig. 4 The dimensionless natural frequency versus the length-to-thickness ratio $l_{\rm a}/h$ for different values of the power index (color online)

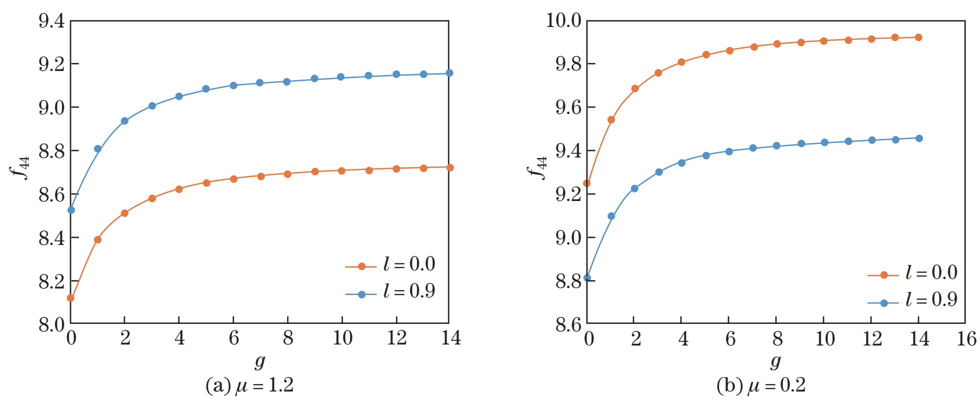

Fig. 5 The dimensionless natural frequency ($f_{44}=\Omega_{44}$) versus the FG power index (color online)

Figure 6 shows the parameters A_{11}, A_{12}, and A_{13} as a function of the FG power index. It is clear that the parameters have maximum values for the FG power index g, and the parameters decrease with the increasing values of g.

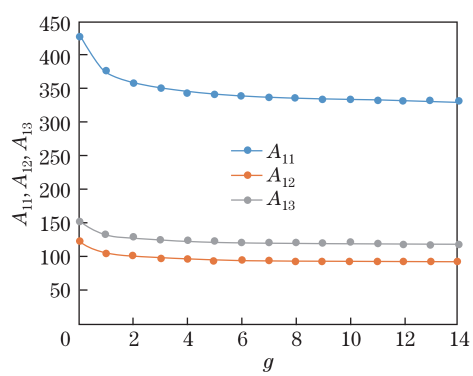

Fig. 6 Variations of the parameters A_{11}, A_{12}, and A_{13} as a function of the FG power index (color online)

Figure 7 shows the dimensionless natural frequency of the FGP nanoplate versus the surface area ($l_\mathrm{a}l_\mathrm{b}$) for two different shapes of square and rectangle with $h = 5$ nm and $\mu = 1$. It is obvious that the nanoplate shape has a significant effect on the natural frequency. It is seen that the natural frequency for the square nanoplate has larger values than the rectangular nanoplate.

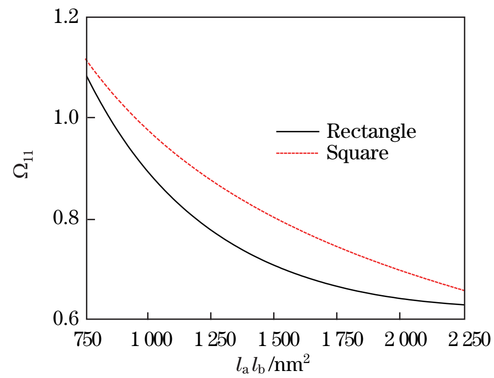

Fig. 7 The dimensionless natural frequency versus the surface area with $h = 5$ nm and $\mu = 1$ (color online)

6 Conclusions

In this work, the vibration behaviors of FGP nanoplates based on the nonlocal strain gradient theory are studied. Using Hamilton's principle, we derive the governing differential equations and then we solve the equations to determine the natural frequencies. We study the effect of various parameters on the natural frequency of FGP nanoplates. The conclusions are summarized as follows.

(i) The natural frequency is a decreasing function of the nonlocal parameter.

(ii) The natural frequency is a decreasing function of the length of the nanoplate for all modes.

(iii) The natural frequency is increased with the FG power index for a fixed length.

(iv) The natural frequency is increased with the aspect ratio $l_\mathrm{a}/l_\mathrm{b}$.

(v) The natural frequency is increased with the FG power index for an aspect ratio.

(vi) With enhancing l_a/h, the nanoplate becomes thinner and thus it has a lesser stiffness.

References

[1] SLADEK, J., SLADEK, V., KASALA, J., and PAN, E. Nonlocal and gradient theories of piezoelectric nanoplates. *Procedia Engineering*, **190**, 178–185 (2017)

[2] LIANG, X., HU, S., and SHEN, S. Bernoulli-Euler dielectric beam model based on strain-gradient effect. *Journal of Applied Mechanics*, **80**, 044502–044508 (2013)

[3] GRAIGHEAD, H. G. Nanoelectromechanical systems. *Science*, **290**, 1532–1535 (2000)

[4] EKINCI, K. L. and ROUKES, M. L. Nanoelectromechanical systems. *Review of Scientific Instruments*, **76**, 061101–061112 (2005)

[5] DEQUESNES, M., ROTKIN, S. V., and ALURU, N. R. Calculation of pull-in voltages for carbon-nanotube-based nanoelectromechanical switches. *Nanotechnology*, **13**, 120–131 (2002)

[6] SAHMANI, S. and FATTAHI, A. M. Small scale effects on buckling and postbuckling behaviors of axially loaded FGM nanoshells based on nonlocal strain gradient elasticity theory. *Applied Mathematics and Mechanics* (*English Edition*), **39**, 561–580 (2018) https://doi.org/10.1007/s10483-018-2321-8

[7] FLECK, N. A., MULLER, G. M., ASHBY, M. F., and HUTCHINSON, J. W. Strain gradient plasticity: theory and experiment. *Acta Metallurgica et Materialia*, **42**, 475–487 (1994)

[8] LI, X. F., WANG, B. L., and LEE, K. Y. Size effects of the bending stiffness of nanowires. *Journal of Applied Physics*, **105**, 074306–074311 (2009)

[9] LI, L., TANG, H., and HU, Y. The effect of thickness on the mechanics of nanobeams. *International Journal of Engineering Science*, **123**, 81–91 (2018)

[10] ZHU, X. and LI, L. On longitudinal dynamics of nanorods. *International Journal of Engineering Science*, **120**, 129–145 (2017)

[11] MINDLIN, R. D. and TIERSTEN, H. F. Effects of couple-stresses in linear elasticity. *Archive for Rational Mechanics and Analysis*, **11**, 415–448 (1962)

[12] KOITER, W. T. Couple stresses in the theory of elasticity. *Philosophical Transactions of the Royal Society of London B*, **67**, 17–44 (1964)

[13] BEVER, M. and DUWEZ, P. Gradients in composite materials. *Materials Science and Engineering*, **10**, 1–8 (1972)

[14] JHA, D., KANT, T., and SINGH, R. A critical review of recent research on functionally graded plates. *Composite Structures*, **96**, 833–849 (2013)

[15] KARAMI, B., SHAHSAVARI, D., and JANGHORBAN, M. Wave propagation analysis in functionally graded (FG) nanoplates under in-plane magnetic field based on nonlocal strain gradient theory and four variable refined plate theory. *Mechanics of Advanced Materials and Structures*, **25**, 1047–1057 (2018)

[16] LI, X., LI, L., HU, Y., DING, Z., and DENG, W. Bending, buckling and vibration of axially functionally graded beams based on nonlocal strain gradient theory. *Composite Structures*, **165**, 250–265 (2017)

[17] LYU, C. F., CHEN, W. Q., and LIM, C. W. Elastic mechanical behavior of nano-scaled FGM films incorporating surface energies. *Composites Science and Technology*, **69**, 1124–1130 (2009)

[18] SEDIGHI, H. M., DANESHMAND, F., and ABADYAN, M. Modified model for instability analysis of symmetric FGM double-sided nano-bridge: corrections due to surface layer, finite conductivity and size effect. *Composite Structures*, **132**, 545–557 (2015)

[19] SEDIGHI, H. M., KEIVANI, M., and ABADYAN, M. Modified continuum model for stability analysis of asymmetric FGM double-sided NEMS: corrections due to finite conductivity, surface energy and nonlocal effect. *Composites Part B*: *Engineering*, **83**, 117–133 (2015)

[20] EBRAHIMI, F., BARATI, M. R., and DABBAGH, A. A nonlocal strain gradient theory for wave propagation analysis in temperature-dependent inhomogeneous nanoplates. *International Journal of Engineering Science*, **107**, 169–182 (2016)

[21] CIVALEK, Ö. Buckling analysis of composite panels and shells with different material properties by discrete singular convolution (DSC) method. *Composite Structures*, **161**, 93–110 (2017)

[22] AKGÖZ, B. and CIVALEK, Ö. Longitudinal vibration analysis of strain gradient bars made of functionally graded materials (FGM). *Composites Part B*: *Engineering*, **55**, 263–268 (2013)

[23] LEE, C. Y. and KIM, J. H. Hygrothermal postbuckling behavior of functionally graded plates. *Composite Structures*, **95**, 278–282 (2013)

[24] EBRAHIMI, F. and BARATI, M. R. Vibration analysis of piezoelectrically actuated curved nano-size FG beams via a nonlocal strain-electric field gradient theory. *Mechanics of Advanced Materials and Structures*, **47**, 350–359 (2018)

[25] SOBHY, M. An accurate shear deformation theory for vibration and buckling of FGM sandwich plates in hygrothermal environment. *International Journal of Mechanical Sciences*, **110**, 62–77 (2016)

[26] JAFARI, A. A., JANDAGHIAN, A. A., and RAHMANI, O. Transient bending analysis of a functionally graded circular plate with integrated surface piezoelectric layers. *International Journal of Mechanics and Material Engineering*, **9**, 8–21 (2014)

[27] JANDAGHIAN, A. A., JAFARI, A. A., and RAHMANI, O. Vibrational response of functionally graded circular plate integrated with piezoelectric layers: an exact solution. *Engineering Solid Mechanics*, **2**, 119–130 (2014)

[28] JANDAGHIAN, A. A., JAFARI, A. A., and RAHMANI, O. Exact solution for transient bending of a circular plate integrated with piezoelectric layers. *Applied Mathematics Modelling*, **37**, 7154–7163 (2013)

[29] ZHANG, S., XIA, R., LEBRUN, L., ANDERSON, D., and SHROUT, T. R. Piezoelectric materials for high power, high temperature applications. *Materials Letters*, **59**, 3471–3475 (2005)

[30] MAHINZARE, M., RANJBARPUR, H., and GHADIRI, M. Free vibration analysis of a rotary smart two directional functionally graded piezoelectric material in axial symmetry circular nanoplate. *Mechanical Systems and Signal Processing*, **100**, 188–207 (2018)

[31] MAHINZARE, M., ALIPOUR, M. J., SADATSAKKAK, S. A., and GHADIRI, M. A nonlocal strain gradient theory for dynamic modeling of a rotary thermo piezoelectrically actuated nano FG circular plate. *Mechanical Systems and Signal Processing*, **115**, 323–337 (2019)

[32] QIU, J., TANI, J., UENO, T., MORITA, T., TAKAHASHI, H., and DU, H. Fabrication and high durability of functionally graded piezoelectric bending actuators. *Smart Materials and Structures*, **12**, 115–121 (2003)

[33] HE, J. and LILLEY, C. M. Surface effect on the elastic behavior of static bending nanowires. *Nano Letters*, **8**, 1798–1802 (2008)

[34] ASGHARI, M., RAHAEIFARD, M., KAHROBAIYAN, M., and AHMADIAN, M. The modified couple stress functionally graded Timoshenko beam formulation. *Material Design*, **32**, 1435–1443 (2011)

[35] ANSARI, R., GHOLAMI, R., and SAHMANI, S. Free vibration analysis of size-dependent functionally graded microbeams based on the strain gradient Timoshenko beam theory. *Composite Structures*, **94**, 221–228 (2011)

[36] RAHMANI, O. and PEDRAM, O. Analysis and modeling the size effect on vibration of functionally graded nanobeams based on nonlocal Timoshenko beam theory. *International Journal of Engineering Sciences*, **77**, 55–70 (2014)

[37] THAI, H. T. A nonlocal beam theory for bending, buckling, and vibration of nanobeams. *International Journal of Engineering Sciences*, **52**, 56–64 (2012)

[38] TOUNSI, A., BENGUEDIAB, S., ADDA, B., SEMMAH, A., and ZIDOUR, M. Nonlocal effects on thermal buckling properties of double-walled carbon nanotubes. *Advances in Nano Research*, **1**, 1–11 (2013)

[39] BENGUEDIAB, S., HEIRECHE, H., BOUSAHLA, A. A., TOUNSI, A., and BENZAIR, A. Nonlinear vibration properties of a zigzag single-walled carbon nanotube embedded in a polymer matrix. *Advances in Nano Research*, **3**, 29–37 (2015)

[40] BENGUEDIAB, S., TOUNSI, A., ZIDOUR, M., and SEMMAH, A. Chirality and scale effects on mechanical buckling properties of zigzag double-walled carbon nanotubes. *Composite Part B: Engineering*, **57**, 21–24 (2014)

[41] ERINGEN, A. C. On differential equations of nonlocal elasticity and solutions of screw dislocation and surface waves. *Journal of Applied Physics*, **54**, 4703–4710 (1983)

[42] ERINGEN, A. C. *Nonlocal Continuum Field Theories*, Springer, Berlin (2002)

[43] ERINGEN, A. C. and EDELEN, D. On nonlocal elasticity. *International Journal of Engineering Sciences*, **10**, 233–248 (1972)

[44] JANDAGHIAN, A. A. and RAHMANI, O. Vibration analysis of functionally graded piezoelectric nanoscale plates by nonlocal elasticity theory: an analytical solution. *Superlattices and Microstructures*, **100**, 57–75 (2016)

[45] EZZIN, H., MKAOIR, M., and AMOR, M. B. Rayleigh wave behavior in functionally graded magneto-electro-elastic material. *Superlattices and Microstructures*, **112**, 455–469 (2017)

[46] ARANI, A. G., KOLAHCHI, R., and VOSSOUGH, H. Buckling analysis and smart control of SLGS using elastically coupled PVDF nanoplate based on the nonlocal Mindlin plate theory. *Physica B*, **407**, 4458–4469 (2012)

[47] KE, L. L., LIU, C., and WANG, Y. S. Free vibration of nonlocal piezoelectric nanoplates under various boundary conditions. *Physica E*, **66**, 93–106 (2015)

[48] TANG, H., LI, L., and HU, Y. Coupling effect of thickness and shear deformation on size-dependent bending of micro/nano-scale porous beams. *Applied Mathematical Modelling*, **66**, 527–547 (2019)

[49] TANG, H., LI, L., HU, Y., MENG, W., and DUAN, K. Vibration of nonlocal strain gradient beams incorporating Poisson's ratio and thickness effects. *Thin-Walled Structures*, **137**, 377–391 (2019)

[50] NATARAJAN, S., CHAKRABORTY, S., THANGAVEL, M., BORDAS, S., and RABCZUK, T. Size-dependent free flexural vibration behavior of functionally graded nanoplates. *Computational Material Sciences*, **65**, 74–80 (2012)